ELSEVIER

International Journal of Mass Spectrometry 209 (2001) 23–29

International Journal of Mass Spectrometry

The energies of the triply excited $n = 2$ intrashell He^- resonances $2s^22p$ and $2s2p^2$ revisited

T. Fiegele[a], N. Mason[b], V. Foltin[c], P. Lukac[c], A. Stamatovic[d], P. Scheier[a], T. D. Märk[a,e,*]

[a]*Institut für Ionenphysik, Leopold Franzens Universität, Technikerstrasse 25, A-6020 Innsbruck, Austria*
[b]*Department of Physics and Astronomy, University College London, Gower Street, London WC1E 6BT, UK*
[c]*Department of Plasmaphysics, Comenius University, Mlynska dolina, 84248 Bratislava, Slovak Republic*
[d]*Permanent address: Faculty of Physics Beograd, P.O.Box 368, 11001 Beograd, Yugoslavia and* [e]*Department of Plasmaphysics, Comenius University, Mlynska dolina, 84248 Bratislava, Slovak Republic*

Received 12 February 2001; accepted 21 March 2001

Abstract

Using a recently constructed high-resolution crossed-beam apparatus consisting of a hemispherical electron monochromator and a quadrupole mass spectrometer, we have measured in detail the He^+ ionization cross-section function in the electron energy range from ~56–59 eV. By fitting the two structures corresponding to the presence of the two triply excited $n = 2$ intrashell He^- resonances $(2s^22p)^2P$ and $(2s2p^2)^2D$ with the theoretical natural line shape, we have deduced that their energy positions lie at 57.06 ± 0.05 and 58.15 ± 0.05 eV, respectively. Between these two states, an additional previously unseen structure has been observed and tentatively linked to the doubly excited autoionizing $(2s^2)^1S$ state of He. When comparing the presently deduced resonance energies with previous data, there is good agreement within the error bars with those experiments which used both a similar experimental technique to detect these states and a data analysis based on the Fano line shape. Experimental results using other methods to detect and characterize these states (electron scattering, electron excitation) appear to lie at slightly higher energies; nevertheless, the energy separation between the two states is the same for almost all experiments. (Int J Mass Spectrom 209 (2001) 23–29) © 2001 Elsevier Science B.V.

Keywords: Electron ionization; resonances; helium; high-energy resolution

1. Introduction

Excitation into quasi-localized states of the continuous spectrum of atomic negative ions has been shown to lead to resonance structures in otherwise smooth reaction rate curves of the corresponding transition process for the production of these atomic negative ions. Resonances in spectra of electrons transmitted through helium in the vicinity of 57 and 58 eV was first discovered by Kuyatt et al. [1] in 1965. These two resonances were interpreted by Fano and Cooper [2] as being caused by the temporary formation of a He^- anion where all three electrons were excited to the $n = 2$ shell with the respective configurations $(2s^22p)^2P$ and $(2s2p^2)^2D$. In the years preceding the reviews by Schulz [3] and Buckman and Clark [4], the energy positions of these two triply excited $n = 2$ resonances were measured in a

*Corresponding author. E-mail: Tilmann.Maerk@uibk.ac.at

PII S1387-3806(01)00436-5

Table 1
Measured energies E_r and energy separation ΔE_r for the two triply excited $n = 2$ intrashell He^- resonances $(2s^22p)^2P$ and $(2s2p^2)^2D$ using different experimental methods including electron transmission (ET), trapped electron (TE), ejected electron (EE), He^+ (ion), metastable (meta), and photon (hv) detection[a]

Authors	Method	E_r for $(2s^2p)^2P$ (eV)	E_r for $(2s2p^2)^2D$ (eV)	ΔE_r (eV)
Kuyatt et al. 1965 [1]	ET	57.1 ± 0.1	58.2 ± 0.1	1.1
Burrow and Schulz 1969 [7]	TE	(56.93 ± 0.1)	(58.04 ± 0.1)	1.11
Grissom et al. 1969 [8]	TE, ion	[57.23 ± 0.05]	(58.04 ± 006]	1.15
Golden and Zecca 1970 [9]	ET	(56.80)	(58.00)	1.20
Quemener et al. 1971 [10]	ion	57.15 ± 0.04	58.23 ± 0.04	1.08
Heidemann et al. 1971 [11]	hv	(57.5 ± 0.5)	(58.7 ± 0.5)	1.2
Sanche and Schulz 1972 [12]	ET	(57.16 ± 0.05)	(58.25 ± 0.05)	1.09
Marchand 1973 [13]	hv	(57.2 ± 0.05)	(58.3 ± 0.05)	1.1
Preston et al. 1973 [14]	ET	57.11 ± 0.06	58.20 ± 0.06	1.09
Hicks et al. 1974 [15]	EE	(57.22 ± 0.04)	(58.30 ± 0.04)	1.08
Bolduc and Marmet 1975 [16]	meta	57.12 ± 0.02	58.19 ± 0.02	1.07
Roy 1977 [17]	ET	(57.19 ± 0.03)	(58.29 ± 0.03)	1.094
Present article	ion	57.06 ± 0.05	58.15 ± 0.05	1.09

[a] The values in square brackets correspond to results deduced from the dip of the resonance, and the values in round brackets correspond to the center of the resonance without fitting the data with the natural line shape. Not shown in this table is the result of Gosselin and Marmet 1990 [18], as they have only studied the higher resonance yielding a value of 58.283 ± 0.003 eV.

variety of different experiments, including electron-transmission studies; a trapped-electron experiment; and ejected electron, ion, photon, and metastable detection. Moreover, a number of calculations have been carried out, yielding quite differing values for the energy position and the width of these resonances (for details, see data given in [5,6]), with the most recent work [6] applying the complex-coordinate rotation method with large basis sets giving, for the lower resonance, a value of 57.205 eV and a line width of 71 meV and, for the higher resonance, a value of 58.303 eV and a line width of 49 meV, respectively.

Nevertheless, as can be seen from Table 1, there exist discrepancies between experimental values [1,7–18] larger than the combined error bars, and in addition, some of the experimental values are at variance with the most recent theoretical value as given above. As has been pointed out by Heideman et al. [11], one of the reasons for these discrepancies may be errors in the energy calibration. Thus, despite a large number of experimental (and theoretical, see [5,6]) studies concerning the position and sometimes the shape of these fundamental compound states in atomic physics, no definitive quantitative answer has been given to date concerning the true position and shape of these resonances.

We recently constructed a high-resolution crossed-beam machine [19,20] to study the inelastic interaction of electrons with atoms, molecules, and clusters in detail, allowing us to determine with high accuracy the threshold behavior of ionization cross sections and to derive corresponding appearance energies [21–23]. This apparatus consists of a specially designed hemispherical electron monochromator, a gas inlet system, and a quadrupole mass spectrometer. For this study, which concerns the energies of these resonances, we have employed additional checks on the energy scale calibration and on the energy resolution in the vicinity of the resonance positions. From the measured high-resolution ionization efficiency curves for He in the energy range between 56 and 59 eV we have deduced values for the energies by fitting the data to theoretical line profiles.

2. Experimental

The apparatus used for these experiments, described in detail previously [19–23], consists of an electron gun, a collision chamber, and an electron collection system. This system was primarily built in our Innsbruck laboratory for the study of electron–particle interactions under high sensitivity and high-energy resolution. Target systems (atoms in this

Table 2
Measured appearance energies for positive ions of some rare gases and molecules, compared (using Xe to calibrate the energy scale) to standard values derived from photoionisation results (taken from NIST [26])

Target	Present AE value (eV)	NIST value (eV)	Difference present-NIST (meV)	p Value
Xe	12.12987	12.12987	0	1.12
Ar	15.749 ± 0.012	15.759 ± 0.001	−10	1.30
Kr	13.990 ± 0.015	13.999 ± 0.001	−9	1.22
H_2	15.424 ± 0.025	15.426 ± 0.00005	−2	1.19
D_2	15.469 ± 0.025	15.467	+2	1.2
N_2	15.590 ± 0.011	15.581 ± 0.008	+9	1.18
O_2	12.073 ± 0.021	12.0697 ± 0.0002	+3	1.24
N_2O	12.865 ± 0.009	12.889 ± 0.004	−24	1.28

study) can either be admitted as a stagnant background gas or enter the collision region via a non-seeded adiabatic expansion of a temperature-controlled gas through a thin orifice of 20 μm diameter at a stagnation pressure of up to several bars. At a distance of 2 cm, the gas beam is skimmed with a 1-mm-diameter skimmer, and 8 cm further downstream, shortly before it interacts with the electrons, the beam is collimated to a diameter of 3 mm. The expansion chamber and the interaction region are separately (differentially) evacuated by 500 l/s turbomolecular pumps.

The monochromatized electrons (with typical currents in this study of ∼50 nÅ, also see below) are produced by a standard home-built hemispherical electron monochromator (HEM), the performance of which has been improved by giving careful attention to a number of technical details. The hemispheres, the sample inlet system, and all electron-ion-optical elements are made of a single material (stainless steel) to improve uniformity of surface potentials. Differential pumping (using turbomolecular pumps) between the different parts and frequent bake-outs are invoked to reduce contamination of the surfaces. Residual magnetic fields in the whole instrument are kept below 0.003 Gauss with Helmholtz coils compensating for the earth's magnetic field. Ferromagnetic materials were avoided in the vicinity of the electron beam. All voltages applied to the electron-ion-optical elements are supplied by a specially constructed power supply with a ripple of ≤1 mV.

Ions formed in the collision chamber are extracted in line with the neutral beam direction by a weak electric field. Usually, a rather low ion-extraction voltage of ∼50 mV (corresponding to an electric field strength of ∼0.12 V/cm) was used to minimize disturbing field effects. The extracted ions are then focused by a system of electrostatic lenses into the entrance of a quadrupole mass spectrometer with a nominal mass range of 2000 amu (atomic mass unit). The mass-selected ions are detected by a channeltron multiplier operated in single-ion-counting mode.

One way to check the performance of the instrument is to measure the Cl^- production via dissociative electron attachment (DEA) to CCl_4 at incident energies, E, close to 0 eV [19,20]. In this case, the width of the zero-energy DEA peak is determined by the convolution of the finite electron beam distribution and the rapidly decreasing s-wave cross-section function, so that the full width at half maximum (FWHM) gives a convenient measure for the energy spread of the electron beam. In this experiment, an improved version of our HEM that was recently developed gave, at best, an energy spread of ∼30 meV. Nevertheless, for the present measurements, an energy resolution of ∼100 meV has been used to achieve electron currents large enough (∼50 nÅ) to obtain ion signals big enough to allow us to study details (resonances) in cross-section curves. The zero-energy Cl^-/CCl_4 peak position was also used for calibration of the energy scale at low energies, including the O^- onset for DEA to CO at ∼9.6 eV (for details, see [19,20]).

In addition, appearance energies for the production of singly charged cations of various test gases (including rare gases and molecular gases, see Table 2) have

been measured and used to support the electron energy scale calibration discussed above, which involves electron attachment. The appearance energies of the product cations were derived using a novel data-handling procedure described in detail in recent publications [21–24]. In short, the measured ionization cross section was fitted with a nonlinear weighted least-squares fit of the raw data using the Marquart-Levenberg algorithm. The fit function $F(E)$ is fitted over an energy range that incorporates the threshold region:

$$F(E) = b \quad \text{if the incident electron energy } E < AE \tag{1a}$$

$$F(E) = b + c(E - AE)^p \quad \text{if the incident electron energy } E > AE. \tag{1b}$$

The fit then involves four parameters: b, the background signal; AE, the appearance energy; a scaling constant c; and p, an exponential factor, which, according to Wannier [25], should be 1.127 in the case of the hydrogen atom (for more details on theoretical predictions for the threshold law, see [23]). The data was fitted over an energy range from below the AE (where the only signal is background) to some 3 eV above AE. As a test of the accuracy of fitting method (and the linearity of the energy scale), the ionization cross sections of some rare gases and some simple molecules were measured and appearance energies for cations were derived. Excellent agreement (within ~10 meV) was found with standard values (NIST database [26]), using Xe as a standard gas to calibrate the energy scale (see Table 2). From these results, we conclude that the present fitting technique gives reliable appearance energies for cations produced by electron-impact ionization and that the estimated accuracy of the energy scale is <10 meV and exhibits a good linearity in the energy range (~0–20 eV) covered by these methods.

Recently, we improved our data-fitting technique by allowing for finite electron distribution, which enabled us to deduce the actual electron energy distribution at the energy position of the appearance energy. For this, we assume that the electron energy distribution is approximately a Gaussian distribution centered around AE, with a FW of ΔE at 1/e. Then the fit function (1b) is numerically convoluted with the electron distribution

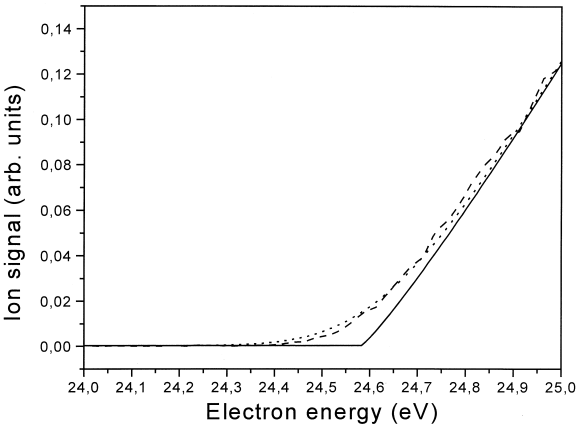

Fig. 1. Electron impact ionization efficiency curve for He close to threshold. Dashed line, experimental data points; full line fit function (1); and dotted line fit function (2).

$$P(E) = \int_{-\infty}^{+\infty} e^{-(E-AE)^2/2\Delta E^2}(b + c(E - AE)^p)dE \tag{2}$$

and compared with the experimental data. This comparison yields information on the experimental FWHM of the electron energy resolution (see Fig. 1, showing the corresponding curves for the ionization of He). The results obtained by this method are similar to results obtained by measuring the s-wave attachment cross section to CCl_4 and, thus, demonstrate that the FWHM of the electron energy distribution of the present machine does not depend on electron energy.

Moreover, for the present task, we have carried out a further check on the reliability of the energy-scale calibration to rule out systematic errors not considered by conventional error analysis (statistical error). In previous studies on the triply excited He resonances, electron energy scales usually have been calibrated at

one rather low energy position. For instance, Quemener et al. [10] and Gosselin and Marmet [18], measuring the He^+ ion yield following high-resolution electron impact, calibrated their energy scale with the spectroscopic value of the He ionization threshold at 24.5876 eV. Sanche and Schulz [12], employing an electron-transmission experiment, calibrated their energy scale using the value of 19.34 ± 0.02 eV for the $(1s2s^2)^2S$ resonance in He after they recalibrated the location of this reference with various thresholds at lower energies. This $(1s2s^2)^2S$ resonance was also used by Preston et al. [14], Hicks et al. [15], and Roy [17]. Burrow and Schulz [7] calibrated their trapped electron tube with the onset for the excitation of the $(2s2p)^3P$ state. In this study, however, we not only carried out multiple checks on the energy scale at and below the He ionization energy but, in addition, we also measured ionization energies of ions with thresholds up to and beyond the energy positions of the triply excited He resonances under study. In particular, we measured the appearance energies of Ar^{2+} and Ne^{2+} ions, and by comparing these results with well-known spectroscopic values [26], we are able to confirm and state that the linearity of the energy scale is fulfilled up to energies of ~60 eV and that possible systematic errors introduced by this are, in our present set-up, on the same order of magnitude as the statistical error of ~10 meV, as determined for the appearance energies of the singly charged ions (see above).

3. Results and Discussion

Fig. 2 shows, as an example, the original data measured for the electron-impact ionization of He via reaction

$$He + e \rightarrow He^+ + 2e \quad (3)$$

in the energy range of the resonances of present interest. This data set has been obtained by summing up 23 successive energy sweeps, each sweep taking ~2800 s to scan 400 channels 5 meV apart from each other. The ionization cross section of He is still increasing with increasing energy in this energy region (see also the absolute measurements in [27]),

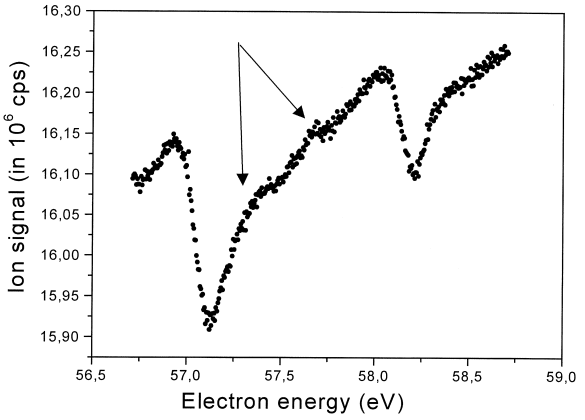

Fig. 2. Ionization efficiency for He as a function of corrected electron energy in the energy range of the two triply excited $n = 2$ intrashell He^- resonances $(2s^22p)^2P$ and $(2s2p^2)^2D$.

but two resonant structures are clearly visible on this scale and, after proper energy calibration (see also Fig. 3), can be clearly identified as being caused by the occurrence of the two triply excited $n = 2$ intrashell He^- resonances $(2s^22p)^2P$ and $(2s2p^2)^2D$. The amplitudes of these structures with ~1.25% and 0.75% of the total ion current, respectively, are similar to the value of 0.8% reported in the earlier measurement by Quemener et al. [10].

After proper subtraction of the slowly rising background ionization signal, the true nature (natural line shape) of the two resonances as predicted by Fano's theory [28] are clearly recognizable in Fig. 3. The cross section for the production of such a negative ion resonance (capture of the incident electron by the neutral He target) can be approximated by the Fano-Cooper formula [2]

$$\sigma(\varepsilon) = a(q + \varepsilon)^2/(1 + \varepsilon^2) + b, \quad (4)$$

where a and b are the resonant and nonresonant cross sections, q is the shape factor and $\varepsilon = (E - E_r)/\Gamma/2$ is the difference between the incident electron energy and the resonance energy E_r in units of the resonance half-width $\Gamma/2$. The FWHM of the structure Γ is related to the lifetime of the state. The shape factor q and the width Γ cannot be deduced from the data without knowledge of the electron energy distribution, as the observed structure corresponds to the

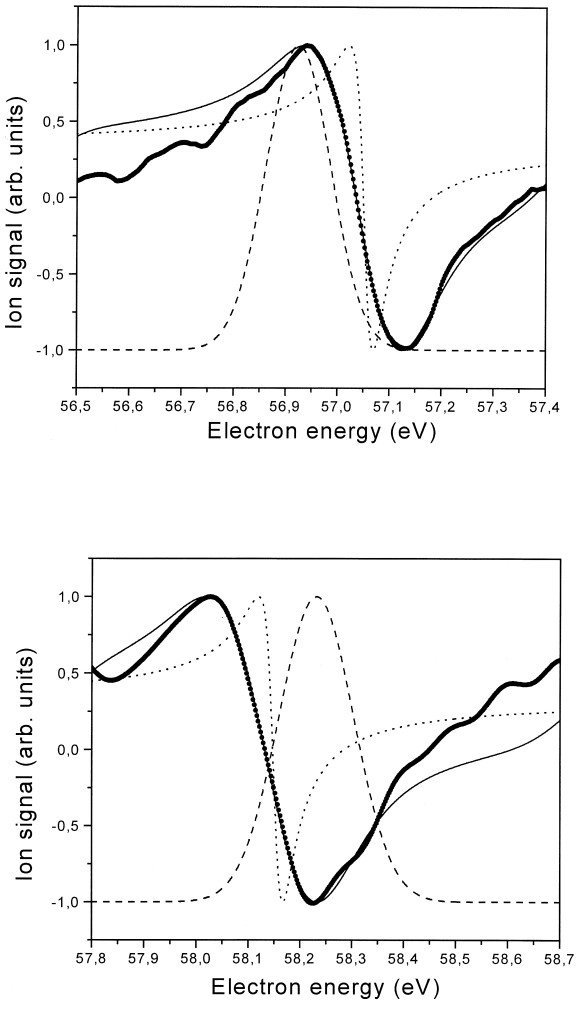

Fig. 3. Measured He^+ ionization-efficiency curve after proper subtraction of the slowly rising background ionization signal (designated full points merging into thick full line) exhibiting the natural line shape of the $(2s^22p)^2P$ (upper panel) and $(2s2p^2)^2D$ (lower panel) resonances. Also shown are the natural line shape (designated by short dashed line) and the electron energy distribution (designated by the long dashed line) used to obtain the best fit (designated by thin full line) to the experimental data.

convolution of this electron energy distribution with the real structure.

Thus in the fitting procedure to deduce Er, we have either started with q and Γ values as deduced earlier by Marmet and coworkers for similar experiments [10,18] or we have started with the Gaussian 100-meV electron energy distribution deduced for the He^+ ionization threshold. In practice, the fit and the resulting E_r is not very sensitive to small variations in these values, and it turns out that an energy distribution of 100 meV gives q and Γ values in close agreement with the earlier determinations. On the other hand, q and Γ values of Quemener et al. [10] (the Γ value corrected by a factor of 2, see [16]) lead to electron energy distributions that are in agreement with the experimentally determined one (thus demonstrating that the energy distribution is not changing for the present instrument with electron energy). Moreover, we have, in accordance with Gosselin and Marmet [18], restricted the energy range of the fit for the higher resonance to account for possible interference caused in the high-energy range by the very narrow $(2s2p)^3P$ resonance at 58.309 eV.

Using this approximation, we obtain for the two triply excited $n = 2$ intrashell He^- resonances $(2s^22p)^2P$ and $(2s2p^2)^2D$ the following E_r values 57.06 and 58.15 eV, respectively. Repeated measurements give similar values within an error bar of 50 meV, including an additional 10 meV for the systematic error bar determined above for the energy scale calibration. These values are in good agreement (within the error bars) with most of the previous high-accuracy experiments. In particular, there is very good agreement within the error bars with those experiments that used both a similar experimental technique to detect these states and a data analysis based on the Fano line shape. Experimental results using other methods to detect and characterize these states (electron scattering, electron excitation) appear to lie at slightly higher energies. It is interesting to note that the energy separation between the two states is, within the error bars, the same for almost all experiments (see Table 1) and, in addition, in very good agreement with the most recent calculation leading to a value of 1.1 eV [6]. This indicates that the difference between previous values obtained by the different experimental methods could be because of the different techniques and energy calibrations used.

It is interesting to note that a simple visual inspection of the experimental data shown in Fig. 2 clearly shows the presence of additional structure—between the resonances not observed previously in ionization efficiency curves—between the approximate energies

of 57.3 and 57.8 eV (as indicated by the two arrows). A similar observation has been reported recently by Gosselin and Marmet [18] for the energy range above the $(2s2p^2)^2D$ resonance and has been identified tentatively with the occurrence of $2p^3$ states. The only known state between the two triply excited $n = 2$ intrashell He^- resonances $(2s^22p)^2P$ and $(2s2p^2)^2D$ is one of the doubly excited states; that is, the autoionizing $(2s^2)\ ^1S$ state at an energy of 57.82 eV with a rather broad width of ~140 meV [7,15]. More accurate measurements are needed to allow definitive identification of this structure.

Acknowledgements

This work was supported partially by the Österreichischer Ionds zur Förderung der wissenschafleichen Forschung (FWF), Wien, Austria, the European Commission, Brussels, and the Austria-Slovak cooperation agreement, project number 29s15.

References

[1] C.E. Kuyatt, J.A. Simpson, S.R. Mielczarek, Phys. Rev. 138 (1965) A385.
[2] U. Fano, J.W. Cooper, Phys. Rev. 138 (1965) A400.
[3] G.J. Schulz, Rev. Mod. Phys. 45 (1973) 378.
[4] S.J. Buckman, C.W. Clark, Rev. Mod. Phys. 66 (1994) 539.
[5] K.T. Chung, Phys. Rev. A22 (1980) 1341.
[6] M. Bylicki, C.A. Nicolaides, Phys. Rev. 51 (1995) 204.
[7] P.D. Burrow, G.J. Schulz, Phys. Rev. Lett. 22 (1969) 1271.
[8] J.T. Grissom, R.N. Compton, W.R. Garrett, Phys. Lett. 30A (1969) 117.
[9] D.E. Golden, Z. Zecca, Phys. Rev. A1 (1970) 241.
[10] J.J. Quemener, C. Paquet, P. Marmet, Phys. Rev. A4 (1971) 494.
[11] H.G.M. Heidemann, W. Van Dalfsen, C. Smit, Physica 51 (1971) 215.
[12] L. Sanche, G.J. Schulz, Phys. Rev. A5 (1972) 1672
[13] P. Marchand, Can. J. Phys. 51 (1973) 814.
[14] J.A. Preston, M.A. Hender, J.W. McConkey, J. Phys. E6 (1973) 661.
[15] P.J. Hicks, S. Cvejanovic, J. Comer, F.H. Read, J.H.M. Sharp, Vacuum 24 (1974) 573.
[16] E. Bolduc, P.Marmet, J. Phys. B 8 (1975) L241.
[17] D. Roy, Phys. Rev. Letters 38 (1977) 1062.
[18] R.N. Gosselin, P. Marmet, Phys. Rev. A41 (1990) 1335.
[19] G. Denifl, D. Muigg, A. Stamatovic, T.D. Märk, Chem. Phys. Lett. 288 (1998) 105.
[20] G. Denifl, D. Muigg, I. Walker, P. Cicman, S. Matejcik, J.D. Skalny, A. Stamatovic and T.D. Märk, Czech. J. Phys. 49 (1999) 383.
[21] D. Muigg, G. Denifl, A. Stamatovic, O. Echt, T.D. Märk, Chem. Physics, 239 (1998) 409.
[22] G. Hanel, T. Fiegele, A. Stamatovic, T. D. Märk, Z. Physik. Chemie, 214 (2000) 1137.
[23] T. Fiegele, G. Hanel, I. Torres, M. Lezius, T.D. Märk, J. Phys. B33 (2000) 4263.
[24] S. Matt, O. Echt, R. Wörgötter, V. Grill, P. Scheier, C. Lifshitz, T. D. Märk, Chem. Phys. Letters 264 (1997) 149.
[25] G.H. Wannier, Phys. Rev. 90 (1953) 817.
[26] W.G. Mallard, P.J. Linstrom, NIST Standard Reference Database E, Vol. 69 (Gaithersburg: National Institute of Standards and Technology) Webpage http://webbook.nist.gov.
[27] T.D. Märk, G.H. Dunn, Electron Impact Ionization, Springer, Wien, 1985.
[28] U. Fano, Phys. Rev. 124 (1961) 1866.